

About the second-order instability on an electrically heated temperature-controlled test section under forced convective boiling conditions

X. C. HUANG and G. BARTSCH

Institut für Energietechnik, TU Berlin, Marchstr. 18, 1000 Berlin 10, Germany

(Received 12 May 1992 and in final form 3 November 1992)

Abstract—During boiling experiments with electrically heated temperature-controlled test sections it was observed by many researchers that although stability conditions can be satisfied in the ordinary sense, wall temperature distribution may tilt over from one form to another quite different form near the CHF and the minimum film boiling conditions. The measured local boiling curves appeared to be discontinuous. By solving the heat conduction problem of the test section with a simplified continuous boiling topography as one of its boundary conditions it is shown that the discontinuous phenomena may be caused by the experimental construction rather than by boiling characteristics. Using an unsteady-state measurement system the two types of second-order instability are observed. Possible ways of getting a fully stable operation of the test section are proposed.

1. INTRODUCTION

TRANSITION boiling is characterized by the negative slope in the boiling curve. Due to this unique heat transfer behavior, steady-state experimental investigations must be carried out with temperature-controlled systems. Among the various methods that have been proposed in the past years, the electrically heated test section with feedback control, which was first used by Peterson [1], has found more and more applications because of a number of advantages [2–6]. The stability criterion, in principle, can be easily satisfied by adjusting the amplification coefficient in the feedback control circuit, also for coolants with high critical heat fluxes and steep slopes in the transition boiling regime.

A problem that electrically heated systems suffer from is that the test section behaves very nonlinearly under forced convective (axial flow) conditions. Transition boiling usually does not appear alone on the heat transfer surface, but coexists with nucleate and/or film boiling. This will cause a large axial temperature gradient and make the data reduction rather difficult. Furthermore, although the stability criterion can be satisfied in the sense of first order (i.e. the reference surface temperature can be kept in the steady-state condition at any given value within the whole boiling regime, including the transition boiling regime), local excursion of the temperature can not be avoided: we call it the second-order instability. It was reported by different authors that once the critical heat flux is exceeded the axial temperature distribution will change drastically from a rather flat to a curved shape and vice versa, although the first-order stability criterion was not violated. Similar phenomena were

also observed near the minimum film boiling point. A direct consequence is that the local boiling curve measured on a given axial position appears to be discontinuous. Large gaps may exist around the CHF and the minimum film boiling points, causing considerable confusion in analyzing and interpreting the experimental results in the literature so far.

The present study is the first systematic effort to clarify this second-order instability phenomenon and to clarify whether it is caused by the boiling characteristic or by the experimental construction.

2. EXPERIMENTAL EVIDENCE

2.1. Observations in the literature

Using an experimental setup including feedback control similar to that of Peterson [1], Johannsen and Kleen [2] carried out a number of experiments at atmospheric pressure with electrically heated wires of different diameters (0.1, 1, 2, 3 mm), heated lengths (10–100 mm) and materials (platinum, nickel). They observed that once the critical heat flux had been exceeded at certain axial location, a stable film boiling region started to build up while the greatest part of the wire was still in nucleate boiling. This means that although the volume-averaged wire temperature can be controlled within the transition boiling regime, large local deviation from this value cannot be excluded. Thus transition boiling in the sense of Berenson's definition as unstable film boiling and unstable nucleate boiling alternately existing at the same location occurred only in a very narrow region.

To restrain this kind of local temperature excursion and thus to expand the transition boiling region they

NOMENCLATURE

a_1, a_2, a_6	weighting coefficients	R_2	outside radius of the test section [m]
B	function form of boiling curve	S	boiling topography
c_p	specific heat capacity [$\text{J kg}^{-1} \text{K}^{-1}$]	T	temperature [$^{\circ}\text{C}$]
F	function form defining reference temperature, equation (5)	T_0	ambient temperature [$^{\circ}\text{C}$]
G	mass flux [$\text{kg s}^{-1} \text{m}^{-2}$]	T_{ref}	reference temperature [$^{\circ}\text{C}$]
h_{fg}	heat of evaporation [J kg^{-1}]	ΔT_{sub}	inlet subcooling [K]
k	heat conductivity [$\text{W m}^{-1} \text{K}^{-1}$]	z	axial coordinate [m]
L	test section length [m]	z_{bc}	axial location for measuring boiling curve [m]
P	pressure [bar]	z_{ref}	axial location for measuring reference temperature [m]
q_{loss}	heat losses [W m^{-2}]	z_1, \dots, z_m	axial measurement locations for building reference temperature, equation (5) [m].
q_{elec}	electrical heat supply [W m^{-2}]		
Q	heat source [W m^{-3}]		
r	radial coordinate [m]		
R_1	inside radius of the test section [m]		

designed an indirectly heated test section with high axial thermal conductance for the inside forced convective flow boiling [2]. The reference signal was taken as the weighted average value of temperature readings of three selected thermocouples located near the heat transfer surface and compared with the set-point voltage. The difference from the comparison is utilized to control the power supply to the test section through an analogue computer. Although stability could be achieved with respect to the set-point signal for all boiling regimes, local excursions of the temperature field were still present in all experiments. It was reported that CHF is reached first in the central region of the test section, a slight increase in the reference temperature will force the axial temperature distribution to change from a rather flat to a curved shape, with nucleate, transition and film boilings coexisting one behind another in the flow direction. At this event, the set-point temperature may be equally satisfied for both wall temperature distributions. Changes from one distribution to another were primarily induced by statistical variations of the controlling parameters of the boiling process.

Weber *et al.* [3] have further improved the above experimental set-up to perform measurements at elevated pressures. The abrupt changes of temperature distribution still exist both at CHF and near the minimum film boiling point in most experimental runs of subcooled boiling. In boiling curves measured at the middle position of the test section there exist discontinuities and gaps, especially in the CHF region [7]. Therefore they speculated that transition boiling does not start from the critical heat flux point, but from another characteristic condition, which was called maximum transition boiling point.

Similar phenomena with distorted boiling curves were also reported by Passos and Gentile [6] on a directly heated temperature-controlled Inconel tube for the study of subcooled boiling in a Freon-113 forced flow. The authors stressed that transition boil-

ing was not stabilized in the region immediately after the peak boiling heat flux.

2.2. Further observations

Using the same test section as that of Weber *et al.* [3, 7], which is sketched in Fig. 1 with $R_1 = 4.85$ mm, $R_2 = 16$ mm and $L = 50$ mm, the present authors have repeated several above mentioned steady-state experiments with the purpose of examining the second-order instability in detail, especially its effect on the measured local boiling curves at different axial positions. Data reduction was performed with a numerical method for solving two-dimensional inverse heat conduction problems [8]. Local boiling curves can be obtained by simply combining the calculated local surface temperature and the radial heat flux. One such experimental result is presented in Fig. 2. It can be seen that except for the boiling curve at

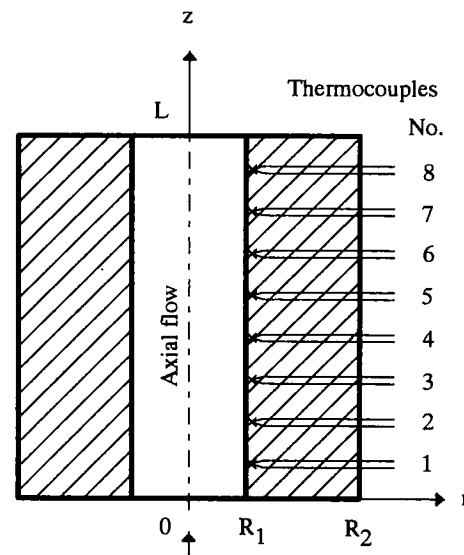


FIG. 1. Sketch of the test section and thermocouple locations.

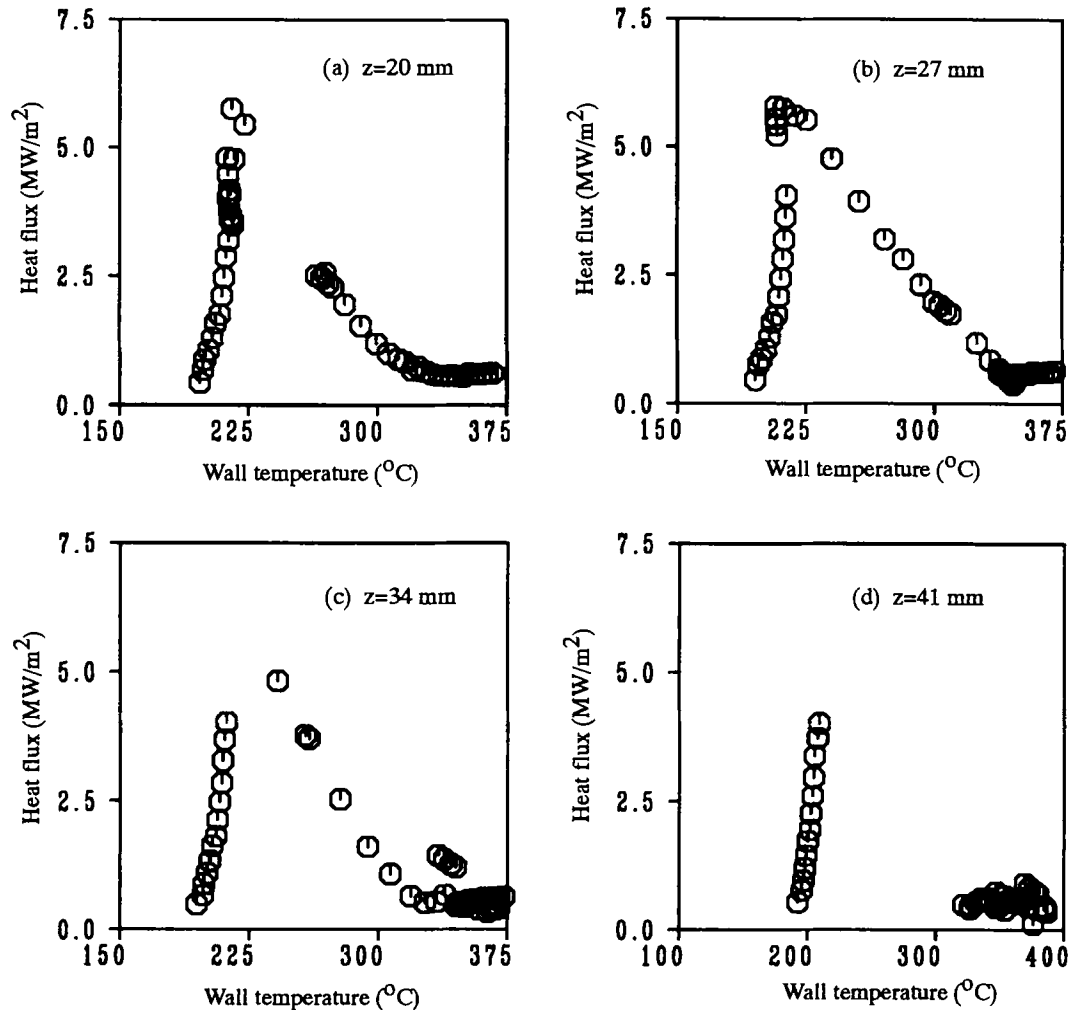


FIG. 2. Effect of the second-order instability on boiling curves measured at different axial positions ($p = 10$ bar, $G = 100$ kg s $^{-1}$ m $^{-2}$, $\Delta T_{\text{sub}} = 30$ K).

the middle position of $z = 27$ mm, which seems quite complete, all boiling curves at the other three axial positions show large gaps of different forms, which correspond to the two second-order instabilities near the CHF and the Leidenfrost point. It is worth noting that the maximum heat flux, which can be reached in the nucleate boiling regime, and the maximum heat flux from which the transition boiling regime begins in Figs. 2(c) and (d) are much less than the critical heat flux in Fig. 2(b).

The temperature excursions and their directions caused by the two second-order instabilities can be seen more clearly by examining the axial temperature distributions of the above measurement. As is shown in Fig. 3, in the first tilt-over of the temperature field at the CHF point the temperature at the test section outlet has increased by as much as 104 K while the temperature at the inlet portion of the test section has decreased by about 11 K. Inversely, in the second tilt-over near the minimum film boiling point temperature at the outlet portion has decreased by 14 K while that

at the inlet portion has increased by 19 K. The same phenomena could also be observed when boiling curves were traversed in the opposite direction, i.e. with decreasing wall temperature. The hatched regions, therefore, represent those that can never be reached, no matter how slowly the reference temperature may be adjusted to change.

The steady-state experiments must be performed very slowly, either step-wise or ramp-wise. Data for a measurement point are usually the average value of a number of measurements taken in a measurement duration, which may be as long as 1 min. The aforementioned tilt-over of temperature field usually begins and ends between two measurement points. However, as the test section always has a finite thermal inertia, no thermal process on it could actually happen jump-wise in transient point of view.

So we have tried to observe the second-order instability of the temperature field using a transient measurement technique on the same test section. Figure 4(a) shows the first type of tilt-over occurring after

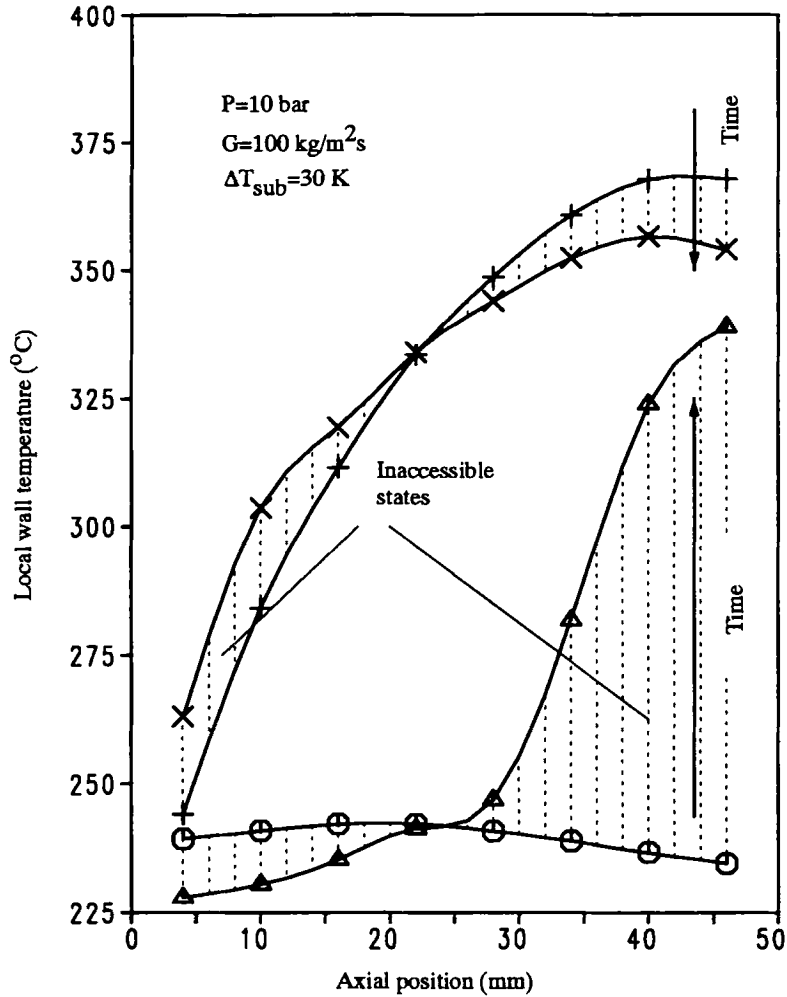


FIG. 3. Abrupt change of temperature distributions in forward measurement on an electrically heated temperature-controlled test section for upflow boiling.

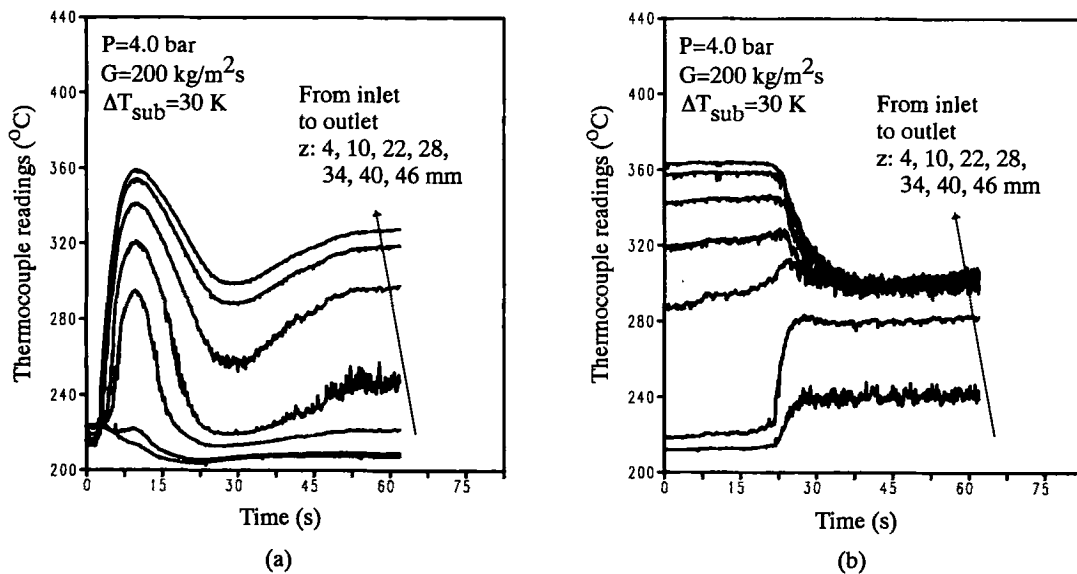


FIG. 4. Wall temperature traces during the two types of second-order instability.

the critical point has been exceeded at the outlet. Once the critical condition (CHF) was first reached at the outlet, it extended very quickly into most of the heat transfer surface because of the unstable nature of the transition boiling and the time lag of the control system. To keep the reference temperature at the set-point value, which was allowed to increase very slowly, the control system began to cut back the power supply, and temperatures began to decrease in all axial positions. After a short period of recovery, a new equilibrium condition was reached. In the newly established steady-state, boiling at the inlet was still in the nucleate boiling regime, but at some lower temperatures, while the temperature at the outlet has increased by as much as 100 K, approximately at the minimum film boiling point. Before and after this event, however, the reference temperature was almost the same.

During the second type of tilt-over shown in Fig. 4(b) the wall temperatures at the test section inlet began to increase, while those at the outlet began to decrease. As a result, nucleate boiling at the inlet has changed to transition boiling, and the higher temperature transition boiling at the outlet has changed to lower temperature transition boiling. This can be recognized by the increased fluctuation amplitude of local wall temperatures.

The first type of tilt-over which lasted about 1 min caused the transition from a uniform axial temperature distribution (nucleate boiling) to a strongly nonuniform distribution (nucleate, transition and film boiling coexisting one after another). The second type of tilt-over which lasted only 20 s caused the latter to change again to another relatively uniform temperature distribution (transition and/or film boiling).

In the following sections we will try to find the physical reason for this second-order instability phenomenon.

3. MATHEMATICAL DESCRIPTION

3.1. The original problem

We observe now a cylindrical test section of length L , inside diameter $2R_1$ and outside diameter $2R_2$, heated uniformly at the outside cylindrical surface, with the coolant flowing upward through the inside channel (Fig. 5). Different boiling modes may occur at different power levels which are controlled according to the set-point value for the reference temperature of the test section.

Assuming constant thermal properties, the heat conduction problem within the test section is described by the parabolic differential equation:

$$\frac{1}{r} \frac{\partial T}{\partial r} \left(r \frac{\partial T}{\partial r} \right) + \frac{\partial^2 T}{\partial z^2} + \frac{Q}{k} = 0, \quad (1)$$

with the following conditions:

$$-k \frac{\partial T}{\partial z} \Big|_{z=L} = q_{\text{loss}}[T(L, r)], \quad (2)$$

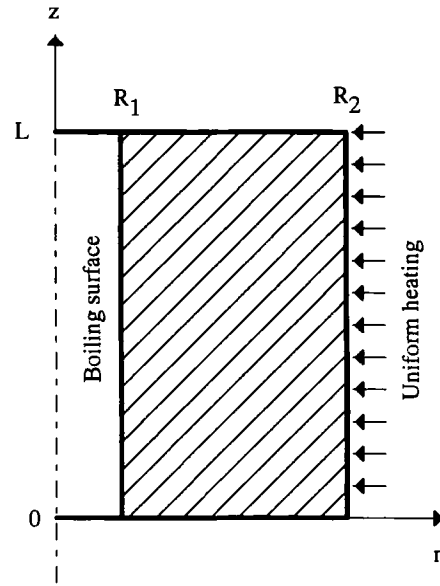


FIG. 5. Diagram of temperature-controlled test section as a heat conducting body.

$$-k \frac{\partial T}{\partial z} \Big|_{z=0} = q_{\text{loss}}[T(0, r)], \quad (3)$$

$$\frac{\partial^2 T}{\partial r \partial z} \Big|_{r=R_2} = 0, \quad (4)$$

$$F[T(R_1, z_1), T(R_1, z_2), \dots, T(R_1, z_m)] = T_{\text{ref}}, \quad (5)$$

$$-k \frac{\partial T}{\partial r} \Big|_{r=R_1} = -S[T(R_1, z), x], \quad (6)$$

with the thermodynamic equilibrium quality defined as:

$$x = \frac{2}{R_1 G h_{\text{fg}}} \int_0^z -k \frac{\partial T}{\partial r} \Big|_{r=R_1} dz - \frac{c_p}{h_{\text{fg}}} \Delta T_{\text{sub}}.$$

Equation (4) defines the axial uniformity of heat supply at the right boundary $r = R_2$. Note that there are two boundary conditions on the heat transfer surface $r = R_1$. The first one (equation (5)) describes the way of forming the reference temperature T_{ref} from measurements at different axial locations z_1, z_2, \dots, z_m . In ref. [3], for instance, the reference temperature is taken as the weighted average value of the three thermocouple readings near the heat transfer surface. Neglecting the small radial distances between these thermocouples and the heat transfer surface, it can be explicitly written as:

$$F[T(R_1, z_1), T(R_1, z_2), \dots, T(R_1, z_m)] = a_2 T(R_1, z_2) + a_4 T(R_1, z_4) + a_6 T(R_1, z_6), \quad (7)$$

where z_2, z_4 and z_6 are axial locations of three thermocouples used for forming the reference temperature, which may be referred from Fig. 1.

The second boundary condition (equation (6)) describes the boiling heat transfer and is the most

complicated one. This results on the one hand from the strong nonlinear dependence of the heat transfer rate upon the surface temperature (boiling curve), and on the other hand from the variation of heat transfer rate with local vapor quality which increases continuously in the flow direction. As the void fraction is practically very difficult to measure, we use the thermodynamic equilibrium vapor quality instead. The function $S(T, x)$ is called boiling topography, which was first suggested by Nelson [9] in order to rule out the confusion accompanying the classical boiling curve. The boiling topography is usually very complex. For simplicity we construct it as the linear projection surface from the saturated vapor point with zero heat flux to the boiling curve at the saturation condition, as illustrated in Fig. 6, i.e.

$$S(T, x) = (1-x)B\left(\frac{T}{1-x}\right), \quad (8)$$

where $B(T)$ is the boiling curve for saturated liquid with zero vapor quality.

Heat losses to the surrounding at the upper and lower ends of the test section through natural convection are taken into account by equations (2) and (3). In the following calculations we assume constant heat transfer coefficients, i.e.

$$q_{\text{loss}}[T(L, r)] = \alpha_u [T(L, r) - T_0], \quad (9)$$

$$q_{\text{loss}}[T(0, r)] = \alpha_l [T(0, r) - T_0], \quad (10)$$

where α_u and α_l are heat transfer coefficients at the upper and lower ends of the test section, respectively.

As the main information of the boundary condition is given at the inner boundary, the present problem is a special kind of inverse problem. The discretized form of equation (5) further increases its complexity. An analytical solution seems therefore impossible, at least to the authors' knowledge. Therefore we will try to reformulate the problem and seek a numerical solution.

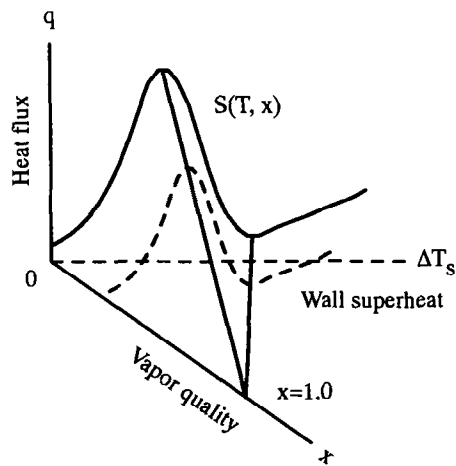


FIG. 6. The simplified boiling topography.

3.2. Reformulation of the problem

The abrupt change of temperature distribution at some set-point values for the reference temperature can be stated as the fact that equation (1) has more than one solution under certain boundary conditions or its solution does not depend continuously on T_{ref} of equation (5). Instead of solving this difficult discontinuity problem directly, we will try to change it into a continuous one by replacing equations (4) and (5) by a single boundary condition:

$$-k \frac{\partial T}{\partial r} \Big|_{r=R_2} = -q_{\text{elec}}, \quad (11)$$

which represents the uniform electrical heat flux at the outer boundary.

The solution of the original problem can be obtained by studying the characteristics of the function $F[T(R_1, z_1), T(R_1, z_2), \dots, T(R_1, z_m)]$ of equation (5) in the reformulated problem.

4. NUMERICAL SOLUTION

Although the differential equation (equation (1)) and the most part of the boundary conditions (equations (2), (3), (11)) are linear, the nonlinear boiling curve and the integral dependence of the local vapor quality on the axial heat flux distribution (equation (6)) cause the problem to be strongly nonlinear. The discretization of the problem was carried out with the difference scheme on a space-grid of 15×10 , and was solved using Newton's method. The integral dependence of the local vapor quality can be quasi-linearly taken into consideration during iteration by calculating it from the result of the last step. The geometrical dimensions are chosen corresponding to the test section used by Weber *et al.* [3] for the steady-state experiment ($L = 50.0$ mm; $R_1 = 4.85$ mm; $R_2 = 16.0$ mm). The smooth boiling curve $B(T)$ is built by referring to CHF and Leidenfrost points available in the literature [7, 10], described with a spline function of third order. Figure 7 demonstrates the three solutions at 10 bar pressures, $100 \text{ kg s}^{-1} \text{ m}^{-2}$ mass flux and 30 K inlet subcooling, corresponding to the same heating heat flux of 45 W cm^{-2} at the outer boundary. To make the comparison clear, heat losses to the surrounding were taken to be zero. This will ensure that the same amount of heat is transferred to the coolant in all three cases.

It is worth noting that for the pool boiling where there is no axial dependence the three solutions must be the same, except at different temperature levels. But for the forced convective case they are quite different. In the nucleate boiling regime (Fig. 7(a)) the axial temperature distribution is very uniform (variation less than 5 K). However, a temperature increase of about 100 K from inlet to outlet can be seen in the solution of transition boiling (Fig. 7(b)). The concentration of isothermals in the inlet area demonstrates the large radial heat flux at the heat transfer

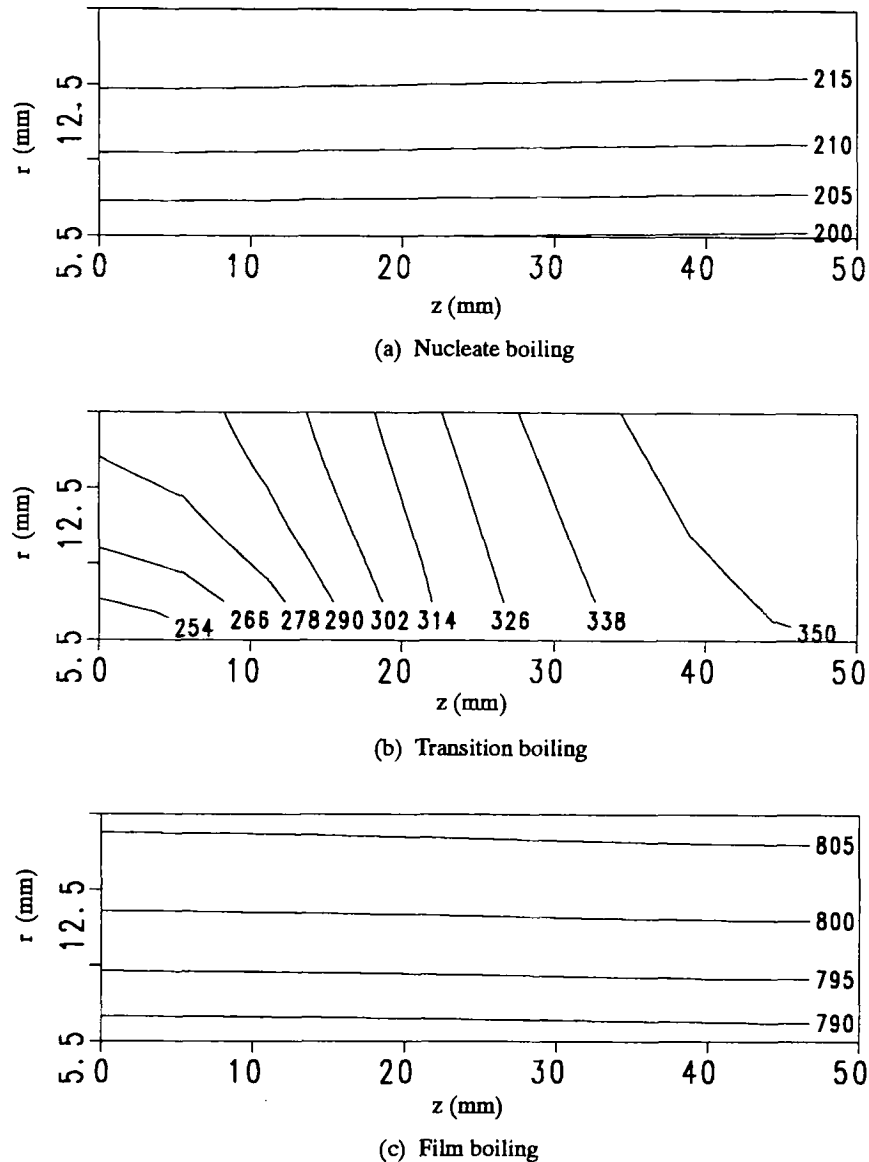


FIG. 7. Temperature fields in different boiling regimes (numbers marking isothermals are in °C).

surface, where low-temperature transition boiling or nucleate boiling occurs. Transition boiling is actually present only in a small region. The axial temperature distribution in the film boiling regime is also very uniform (Fig. 7(c)).

In Fig. 8 axial temperature and heat flux distributions for the same electrical heat supply but for different wall thickness (I.D. remains unchanged) are shown.

The solution of the present model shows several interesting trends that are supported by the experimental observations in the literature and those of ourselves:

(1) If nucleate boiling occurs on the whole heat transfer surface, surface temperature will slightly decrease from inlet to outlet. When transition boiling

already exists on the outlet part of the test section, as can be seen from Fig. 8(a), the nucleate boiling part still shows the same decreasing trend. This seems to be explained by the decreasing critical heat flux temperature with increasing vapor quality, as is reflected in the boiling topography description in equation (8).

(2) For an average heat flux which lies between CHF and the minimum film boiling heat flux, there are generally three boiling modes which can satisfy the steady-state heat balance, i.e. nucleate, transition and film boilings. But unlike the other two boiling modes, transition boiling usually shows a rather complex picture: it doesn't always appear alone, but simultaneously with nucleate or film boiling or both. This will make the heat flux distribution on the boiling surface rather nonuniform, as is shown in Figs. 7 and 8. The transition from one mode to another may be a

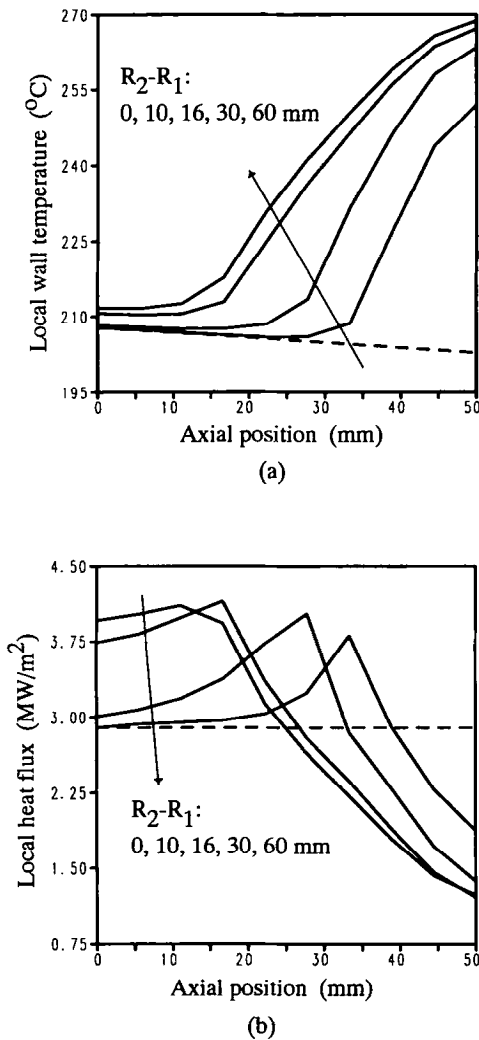


FIG. 8. Axial temperature and heat flux distributions in dependence of wall thickness.

jump-wise process depending on how the reference temperature is built up in the control system for a specific test section, as will be discussed in the subsequent section.

(3) Wall thickness ($R_2 - R_1$) or the axial conductance affects strongly the extension of transition boiling regime. For the same heat flux, as shown in Fig. 8, the local CHF point moves towards the outlet as the wall thickness decreases, restricting transition boiling to a smaller region. Thus a thin-walled tube is not suitable for performing transition boiling experiments, although in principle transition boiling which satisfies steady-state heat balance still exists.

Let us consider two theoretical extreme cases. If the wall thickness approaches zero, there will be no axial conduction at all. Heat flux distribution will be uniform. The solution for transition boiling will become indefinite. Any combination of the isolines of the boiling topography constitutes a solution, i.e.

$$(1-x)B\left(\frac{T}{1-x}\right) = \text{constant}. \quad (12)$$

The solution given in Fig. 8 in dotted lines for zero wall thickness is only one of the infinite possibilities (pure nucleate boiling). This extreme case explains why CHF and post-CHF boiling may appear on relative random locations on thin-walled electrically heated stripes or thin wires, causing local hot spot in transition boiling regime [1, 2].

If the wall thickness is extremely large, the test section will become approximately an isothermal body, transition boiling can be achieved on the whole heat transfer surface. This is, however, in the practice restricted, as the dynamic response has to be properly considered.

Heat losses at both ends of the test section will further deform the temperature fields, especially for the post-CHF region. Calculations, however, have shown that they are not the dominant factor. For the sake of limited space, it will not be discussed here in detail.

5. SECOND-ORDER INSTABILITY ON ELECTRICALLY HEATED TEMPERATURE-CONTROLLED TEST SECTION

Having got the solution under the boundary condition equation (11), we can now study the characteristics of the solution of the original problem defined in Section 3. As the solution of the temperature field depends continuously on the boundary condition equation (11), we need only to consider the relation between equations (5) and (11), i.e. between T_{ref} and q_{elec} .

We consider now three different ways of forming the reference temperature:

- (1) $T(R_1, 0) = T_{ref}$: Wall temperature at inlet as reference temperature.
- (2) $T(R_1, L) = T_{ref}$: Wall temperature at outlet as reference temperature.
- (3) $(T(R_1, 0.23L) + T(R_1, 0.55L) + T(R_1, 0.67L))/3 = T_{ref}$: Reference temperature similar to that used in ref. [3].

For the first case, as is shown in Fig. 9(a), the reference temperature increases monotonously with increasing power supply up to some value near the CHF temperature, and then, after CHF occurs at the outlet, it begins to decrease until the power supply reduces to about one half of its CHF value. Thereafter it increases continuously into the film boiling regime. This means that for a set-point value of T_{ref} in this small domain there are three solutions satisfying the same boundary condition equation (5). As the set-point value for the reference temperature cannot be controlled to follow exactly this up-and-down trace in the experiment, tilt-over of the temperature field will occur at some critical values. For the forward experiment with increasing wall superheat temperature field will jump from point A to B (Fig. 9(a)),

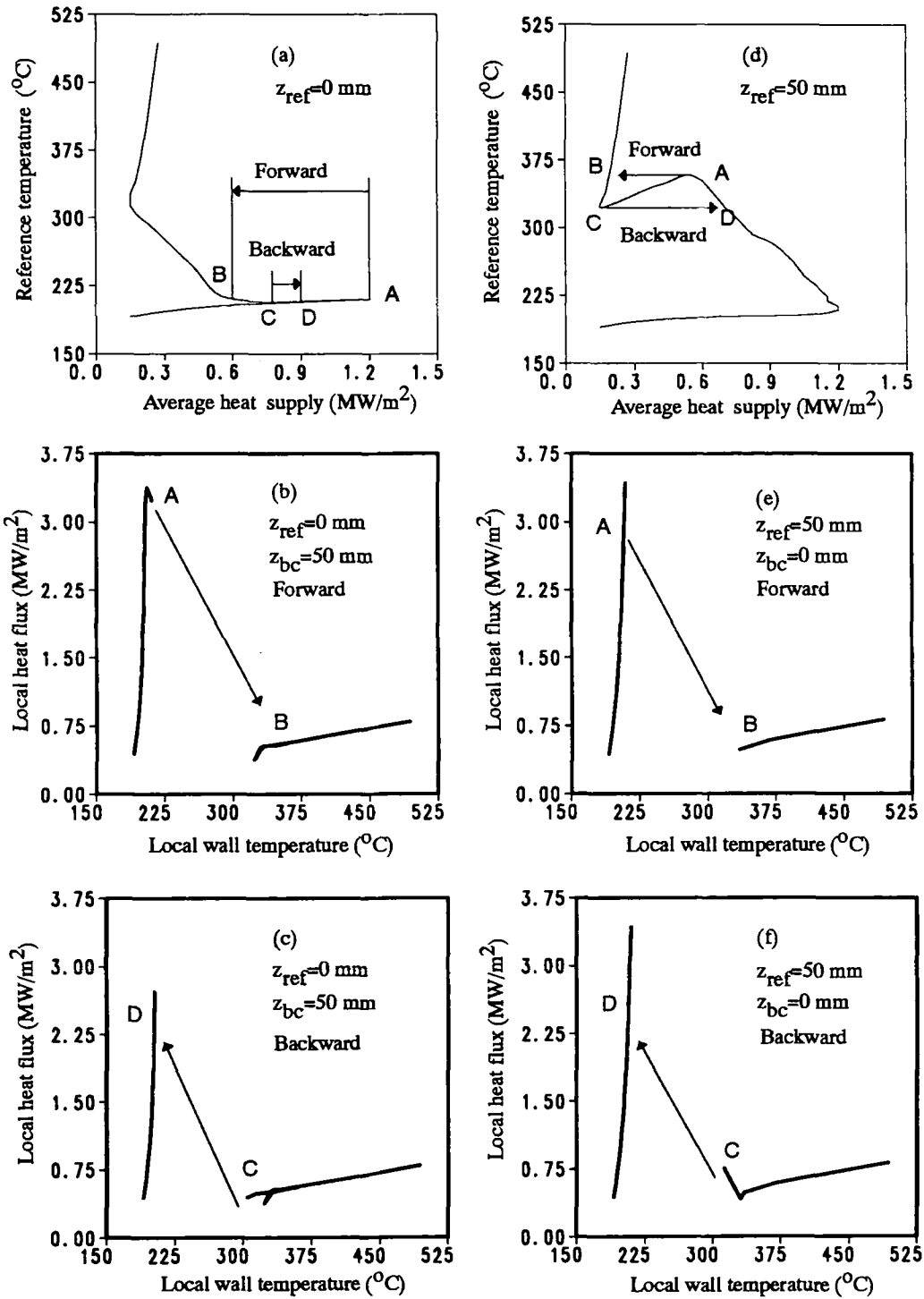


FIG. 9. Characteristics of reference temperatures and the corresponding measurable boiling curves at inlet and outlet of the test section.

causing a gap or discontinuities in the local boiling curve. The most affected position is at the test section outlet, which is shown in Fig. 9(b). For the backward experiment similar phenomenon will happen from point C to D. The corresponding boiling curve is given in Fig. 9(c).

For the second case, the second-order instability occurs near the minimum film boiling temperature, where the reference temperature decreases strongly after it has reached an extreme value at point A and transition boiling has propagated to the test section inlet (Fig. 9(d)). In this case the most affected local

boiling curve is that at test section inlet which is illustrated in Figs. 9(e) and (f) for the forward and backward measurements, respectively.

It is interesting to note in Fig. 9 that forward and backward tilt-overs do not follow the same path. This results in the fact that boiling curves obtained with forward and backward measurements may show quite different pictures, as can be seen by comparing Figs. 9(b) and (c) for the first case discussed above.

It is also worth noting that the peak heat fluxes of local boiling curves in nucleate and transition boiling regimes at different axial positions as well as for different directions of carrying out the experiment are not necessarily the same. In our first case, for example, the critical heat flux condition can be reached at the outlet, but it is not the case for the backward measurement. The peculiar branch of the boiling curve in Fig. 9(c) just before the jump point C is also the calculation result. The seemingly quite confusing pictures which are predicted by the present model agree well with the experimental evidence discussed in Section 2.

The third case is intended to simulate the steady-state experiments conducted by Weber *et al.* [3]. There are, however, several difficulties to do it very satisfactorily. First, it is impossible for us to know exactly the weighting coefficients for the three thermocouple readings used for forming the reference temperature; secondly, the real situation was further complicated by the composite structure of the test section (Monel tube serving as the flow channel and discrete locations of heating elements). Therefore, we consider here only the simplest possible case, i.e. forming the reference temperature by taking the average value of the three thermocouple readings. Despite the simplifications, the predicted trace of the reference temperature does show the potential instability in the CHF and the minimum film boiling regions because of the two rather flat portions shown in Fig. 10(a), where the total change of reference temperature is less than 10 K, while the temperature change at the outlet is as large as 90 K. The predicted trend agrees qualitatively well with the forward measurement shown in Fig. 10(b).

6. WAYS OF ACHIEVING FULLY STABLE OPERATIONS

In the steady-state point of view a good behavior of the temperature-controlled test section is characterized by (1) stable operation in CHF and post-CHF region, also in the sense of second order, i.e. no tilt-overs of temperature field, and (2) relative uniform axial temperature distribution.

The first criterion requires that for a given reference temperature there should be one stable solution only, and that the rate of change of the reference temperature with respect to the heat supply should be as large as possible. Referring again to Figs. 9(a) and (d) we see that if we take the wall temperature at the inlet as the reference temperature this criterion cannot be

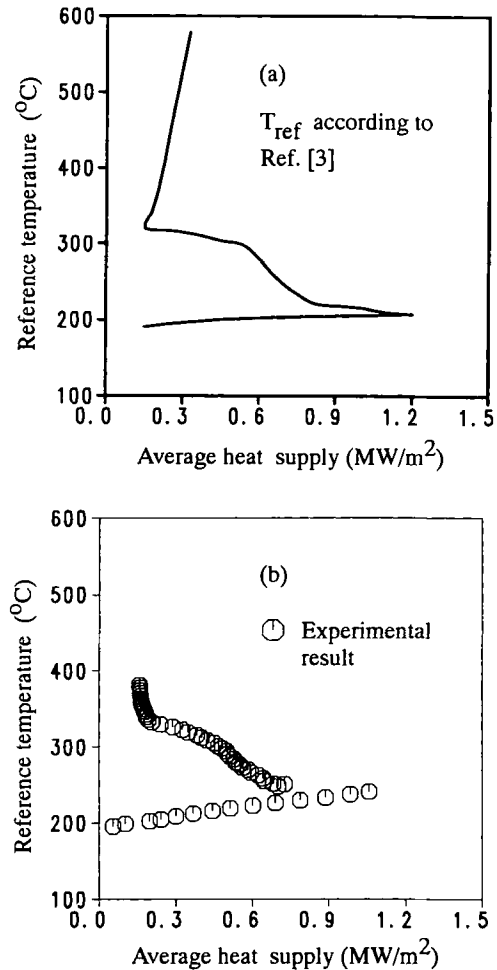


FIG. 10. Comparison of the predicted and measured traces of the reference temperature ($p = 10$ bar, $G = 100$ kg s⁻¹ m⁻², $\Delta T_{\text{sub}} = 30$ K).

satisfied in the lower temperature transition boiling region, as was discussed above, but very well satisfied for the higher temperature post-CHF regions. Inversely, if we take the wall temperature at the outlet as the reference temperature the test section behaves very stable up to the minimum film boiling region (at the outlet), but second-order instability will occur thereafter. As the wall temperatures between the inlet and outlet vary between the two cases, it seems that it will give a better behavior to form the reference temperature from measurements at both the inlet and the outlet (of the heated length), which have the largest sensitivities for high and low temperature boiling regimes, respectively. In fact, as shown in Fig. 11(a), a simple average of the two already gives an excellent characteristic, by which the second-order instability or local temperature excursion can be totally eliminated. Boiling curves can be therefore continuously traversed at all axial positions, as is exemplified in Fig. 11(b).

In the above discussions wall temperatures at the inlet and the outlet are used, simply for the purpose to demonstrate the results more clearly, as measurements

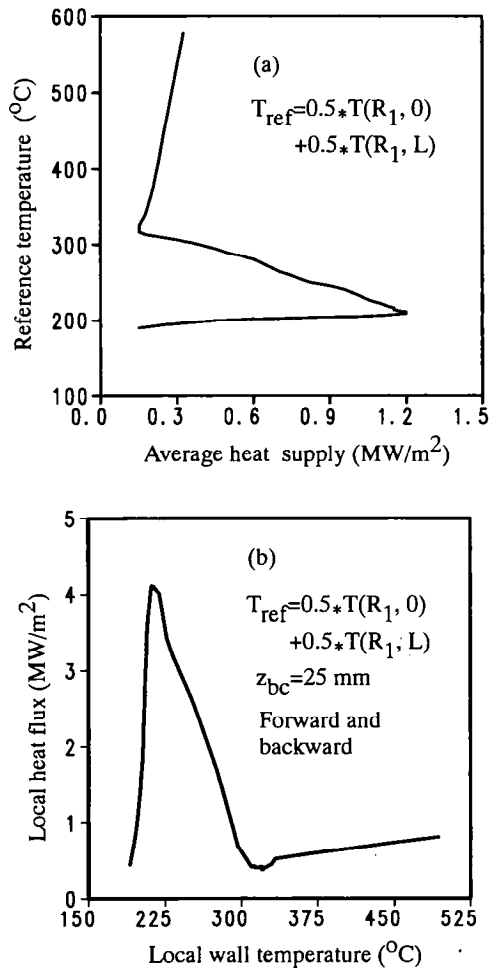


FIG. 11. Reference temperature as an average value of measurements near the inlet and outlet and the obtainable complete boiling curve at a middle position.

on these two locations are most sensible to the power supply. It is, however, quite obvious that in practice, due to physical and instrumental reasons, no thermocouples can and should be located just at the inlet or the outlet, but in a reasonably small distance.

With respect to the second criterion it is better, as suggested by Fig. 8 in Section 4, to use thick-walled test section. This will increase the axial conductance and thus the extension of the transition boiling region. A drawback that comes with this is the increase of the thermal lag in the control system, which may cause failure in the CHF event. One possible way to avoid it is to install heating elements not far from the heat transfer surface despite the increase of the test section outside diameter. The thermal capacity outside the heating elements can help to increase the axial heat conductance without increasing considerably the thermal capacity for the radial heating.

7. CONCLUSIONS

(1) By assuming a continuous boiling topography the proposed model shows that the second-order

instability may occur on the electrically heated temperature-controlled test section for studying forced convective boiling heat transfer if the reference temperature for the control system is not properly formed, which seems to be well supported by our own experiments and those reported in the literature so far. The often observed peculiar forms of local boiling curves, i.e. discontinuities and gaps can also be reasonably explained.

(2) Tilt-over of temperature field in the forward and backward measurements does not necessarily coincide with each other.

(3) The two typical types of tilt-overs of temperature field were observed in transient measurement. It was clearly demonstrated how boiling conditions at individual axial positions changed from one stable condition to another.

(4) To achieve a fully stable operation of the temperature-controlled test section, reference temperature should be formed using temperature measurement near both inlet and outlet of the heated length. Using measurements in the middle positions will reduce the sensitivity of the control system or even lead to second-order instabilities.

REFERENCES

1. W. C. Peterson, A comparator bridge circuit, *IEEE Transaction on Industrial Electronics and Control Instrumentation* IECI 16 (1969).
2. K. Johannsen and U. Kleen, Steady-state measurement of forced convection surface boiling of subcooled water at and beyond maximum heat flux via indirect Joule heating of a test section of high thermal conductance. In *Multi-Phase Flow and Heat Transfer III, Part B: Applications* (Edited by T. N. Veziroglu and A. E. Bergles). Elsevier Science Publishers B.V., Amsterdam (1984).
3. P. Weber, Q. Feng and K. Johannsen, Study of convective transition boiling heat transfer in a vertical tube with slightly subcooled water at medium pressure, *Proc. 5th Miami Intern. Symp. on Multi-phase Transport and Particulate Phenomena*, Miami Beach, Florida, 12-14 Dec. (1988).
4. H. S. Ragheb, S. C. Cheng and D. C. Groeneveld, Observation in transition boiling of subcooled water under forced convective conditions, *Int. J. Heat Mass Transfer* 24, 1127-1137 (1981).
5. H. Auracher, Transition boiling. In *Heat Transfer 1990 (9th International Heat Transfer Conference, Jerusalem, 19-24 August)* (Edited by G. Hetsroni), Vol. 1, pp. 69-96. Hemisphere, New York (1990).
6. J. C. Passos and D. Gentile, An experimental investigation of transition boiling in subcooled Freon-113 forced flow, *J. Heat Transfer* 113, 459-462 (1991).
7. P. Weber, Experimentelle Untersuchungen zur Siedekrise und zum Übergangssieden von strömendem Wasser unter erhöhtem Druck, Ph.D. Thesis, Düsseldorf: VDI Fortschritt-Bericht R3, No. 226 (1990).
8. X. C. Huang, G. Bartsch and B. X. Wang, A numerical method for solving the two-dimensional nonlinear inverse heat conduction problem with application to the study of transient boiling curves. In *Advanced Computational Methods in Heat Transfer, Vol 1: Conduction, Radiation and Phase Change* (Edited by L. C. Wrobel,

- C. A. Brebbia and A. J. Nowak), pp. 381–397. Computational Mechanics Publications, Elsevier Applied Science (1992).
9. R. A. Nelson, Forced-convective post-CHF heat transfer and quenching, *J. Heat Transfer* **104**, 48–54 (1982).
 10. D. C. Groeneveld and K. K. Fung, Forced convective transition boiling: review of literature and comparison of prediction methods, Ontario, Canada, Chalk River Nuclear Laboratories, Report AECL-5543 (1976).